WORLD CONFERENCE ON TIMBER ENGINEERING 2025
BRISBANE, AUSTRALIA
Advancing Timber for the Future Built Environment

RELIABILITY ANALYSIS OF WIND EXCITED TALL MASS-TIMBER BUILDINGS WITH ROCKING POST TENSIONED CROSS LAMINATED TIMBER SHEAR WALLS

Nahom K. Berile[1]; Matiyas A. Bezabeh[2]; Carla Dickof[3]; Md Shahnewaz[4]

ABSTRACT: The design of tall mass-timber buildings is often governed by wind loads due to the light weight and relatively lower stiffness of mass-timber panels compared to their concrete and composite steel equivalents. To maximize the use of mass-timber main wind force resisting systems (MWFRSs), implementing state-of-the-art performance-based wind design (PBWD) approaches is essential. The current code-based wind design of MWFRSs only considers buildings' linear-elastic capacity, resulting in conservative design of timber members and their connections. In contrast, PBWD enables optimal design solutions by allowing nonlinear-inelastic deformation in MWFRS components and corresponding reliability analysis. In this paper, a stochastic simulation-based PBWD framework is implemented to estimate the wind reliability of tall mass-timber buildings with rocking post-tensioned cross-laminated timber (PT-CLT) shear walls. The framework integrates stochastically generated wind tunnel-based load time histories, nonlinear response history analysis (NLRHA) using three-dimensional *OpenSeesPy* numerical models, and a stratified sampling scheme to propagate uncertainties. Full-scale experimental tests of ductile links in PT-CLT walls were conducted at McGill University using newly developed wind-loading protocols to determine their modelling parameters for NLRHA. The framework was implemented to perform structural reliability analysis of a 22-storey prototype wind-excited mass-timber building hypothetically located in Toronto, Canada. The results demonstrate that PT-CLT shear walls provide robust wind resistance, with both system- and component-level collapse reliabilities exceeding target values given in building codes and standards.

KEYWORDS: Reliability analysis; cross laminated timber; timber building; performance-based wind design; wind tunnel test; wind loading.

1 – INTRODUCTION

The design of tall mass-timber buildings is often governed by wind loads due to the light weight and relatively lower stiffness of mass-timber panels compared to their concrete and composite steel equivalents [1, 2]. The current code-based wind design of main wind force resisting systems (MWFRSs) equates the first significant yield with structural failure. This conservative principle can result in costly conservative designs. To maximize the use of mass-timber MWFRSs, implementing state-of-the-art performance-based wind design (PBWD) approaches is essential. Recent advancements in PBWD allow controlled nonlinear-inelastic deformation in specially designed and detailed parts of MWFRSs [3–5]. A core objective of PBWD is to predict the inelastic performance and reliabilities of structures subject to wind loads. As a culmination of several efforts in both the fundamental understanding of nonlinear-inelastic responses of structures under wind [6–11] and the development of wind design frameworks integrating nonlinear-inelastic responses [12–15], the American Society of Civil Engineers (ASCE) has published a pre-standard for PBWD [4, 5].

The ASCE/SEI PBWD pre-standard [5] provides guidelines for wind load characterization, structural response, reliability analysis, and acceptance criteria for MWFRSs and building envelopes. Three performance objectives (POs) are specified in the ASCE/SEI PBWD pre-standard: occupant comfort, operational, and continuous occupancy. For each performance objective, the hazard level is defined in terms of return periods based on the building risk category. The pre-standard states that the MWFRS of a building shall remain elastic for occupant comfort and operational performance objectives. However, inelastic deformation in specific elements or components of the structural system can be allowed in the continuous occupancy state. To ensure that the performance objectives are met, guidelines for evaluating the performance of a structure at global and component levels are also provided. Globally, roof drift and acceleration limits are set, and at the component level, limits on the demand-to-capacity ratio for force- and deformation-controlled elements are provided. A target

[1] Nahom Berile, Department of Civil Engineering, McGill University, Montreal, Canada, nahom.berile@mail.mcgill.ca
[2] Matiyas A. Bezabeh, Department of Civil Engineering, McGill University, Montreal, Canada, matiyas.bezabeh@mail.mcgill.ca
[3] Carla Dickof, Fast + Epp, Vancouver, Canada, cdickof@fastepp.com
[4] Md Shahnewaz, Fast + Epp, Vancouver, Canada, mshahnewaz@fastepp.com

https://doi.org/10.52202/080513-0541

failure probability of 0.0001 has also been given in the pre-standard as an approximation of the target reliability goals specified in ASCE/SEI Standard 7-16 [16]. The pre-standard allows the use of three methods for performance evaluation and reliability analysis. Method 1 uses linear elastic response time history evaluation. Nonlinear time history evaluation for two of the most critical wind directions can be carried out if additional verification of system performance is required. Method 2 relies fully on nonlinear response history analysis for at least 10 wind directions, whereas conditional probability-based reliability assessment is recommended when further analysis is required. Method 3 requires a fully coupled reliability assessment based on limit analysis using shakedown theory [17].

Allowing nonlinear response under wind is challenged by damage accumulation due to the mean component of long-duration along-wind loads. To this end, recent studies have shown that combining self-centring structural systems such as coupled post-tensioned cross-laminated timber (PT-CLT) shear walls and PBWD can limit damage accumulation and result in economic and safe structures [18]. Coupled PT-CLT walls use post-tensioned tendons for overturning moment resistance and self-centring capability, whereas coupling U-shaped flexural plates (UFPs) are used for energy dissipation. In this study, we investigated the wind reliability of tall mass-timber buildings with PT-CLT shear walls using a framework that integrates stochastically generated wind load time histories, nonlinear numerical models, and an efficient stratified sampling scheme.

Reliability analysis of structures under wind loads requires efficient propagation of uncertainty and analysis of extreme nonlinear responses and associated exceedance probabilities using reasonable computational resources. For collapse reliability, the choice of uncertainty propagation technique is even more critical because the estimation of multiple small failure probabilities associated with rare event spaces must be performed within acceptable accuracy. This requirement rules out crude Monte Carlo analysis, which implements a computationally expensive random sampling strategy. Such an approach would require running NLRHA under spatially varying 1-hour duration wind loads for a very large number of samples. To address this limitation, an efficient stratified sampling-based Monte Carlo approach has been proposed [19]. The approach enables simultaneous estimation of multiple failure probabilities in high-dimensional uncertain spaces within preset accuracy limits.

In this paper, wind reliability analysis of a 22-story mass-timber building with PT-CLT shear walls as MWFRSs and hypothetically located in Toronto, Canada, is conducted. To determine the wind speeds at different mean recurrence intervals corresponding to the risk levels given in the ASCE/SEI pre-standard [5], the directional hourly mean wind speed records from Toronto Pearson International Airport station dating from 1953 to 2021 and obtained from Environment Canada were used. The multi-spring numerical modelling approach developed in Berile and Bezabeh [18] using *OpenSeesPy*, which was validated with system-level experiments [20] and full-scale shaking table test results [21], was adopted. Moreover, new modelling parameters for UFPs were determined by conducting experimental tests under newly developed wind-loading protocols. After the design of the prototype building according to the PBWD framework proposed in Berile and Bezabeh [18], a stochastic simulation-based approach was implemented to estimate wind reliabilities.

2- PERFORMANCE-BASED WIND DESIGN OF PT-CLT SHEAR WALLS

PBWD of PT-CLT shear walls incorporating rocking and controlled non-linear inelastic response under design-level wind events was proposed by Berile and Bezabeh [18]. The design approach overcomes the limitations of traditional prescriptive approaches, which equate significant yielding of components of MWFRSs and the decompression state under wind to failure. Details of the design framework can be found in Berile and Bezabeh [18]; the general approach is briefly discussed here.

To properly implement the PBWD approach for the design of coupled PT-CLT shear walls, understanding their response to lateral loads is essential. Under small lateral loads, PT-CLT walls derive their resistance to the overturning effect of lateral loads primarily from initial PT prestressing and gravity loads (Fig. 1(a)). The first critical response to lateral force occurs when the stabilizing effect of gravity loads and initial prestressing is exceeded, leading to the onset of decompression (Fig. 1(b)). Upon further loading, a gap opens at the base of the panels, with subsequent relative vertical deformation of the two panels creating opposite shear forces on the two sides of the coupling UFPs. As the gap opening widens (Fig. 1(c)), these forces reach the yielding capacity of the UFPs, causing inelastic deformation. Further lateral deformation eventually leads to the elastic linear limit (ELL). Beyond the ELL, the overall lateral stiffness of the assembly is reduced, and the wall toe experiences higher compression force, leading to consecutive yielding, splitting, and crushing of the CLT panels.

https://doi.org/10.52202/080513-0541

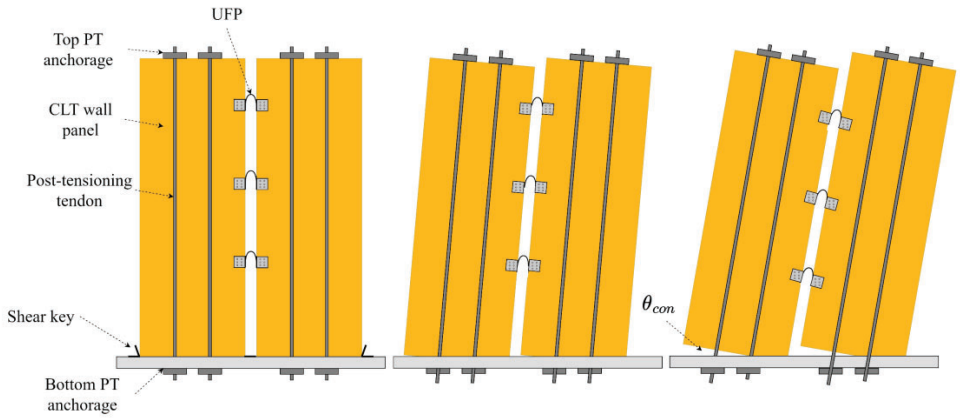

Figure 1. Response of PT-CLT shear walls to lateral loads: a) undeformed shape; b) deformation before onset of decompression; c) deformation beyond decompression (gap opening)

The PBWD framework developed for PT-CLT shear walls [18] is in line with the ASCE/SEI pre-standard [5]. The POs and corresponding acceptance criteria for tall mass-timber buildings with PT-CLT shear walls involve the occupant comfort performance objective (OC-PO), which is associated with limiting building motions and vibrations to minimize occupant discomfort at 1-month, 1-year, and/or 10-year return period wind loads. Corresponding acceptance criteria are frequency-dependent acceleration limits provided in the ASCE/SEI pre-standard [5]. The operational performance objectives (OP-PO) involve limiting the response of PT-CLT walls to the decompression state (no rocking) and ensuring that the building system remains operational. Corresponding acceptance criteria are decompression capacity, peak roof drift, peak residual drift, and peak deformation damage index (DDI) limits. Finally, the continuous occupancy performance objective (CO-PO), which allows the coupling UFPs to undergo limited nonlinear-inelastic responses, requires that the CLT panels and PT bars withstand without any permanent damage. Corresponding acceptance criteria are demand-to-capacity ratios for UFPs, CLT, and PT, as well as global peak roof drift and residual drift limits.

3 – NUMERICAL MODELLING OF PT-CLT SHEAR WALLS

The numerical modelling approach for PT-CLT shear walls developed in [18] is adopted in this study. The model incorporates multiple zero-length parallel springs that represent the compressive behaviour of the timber panel over the rocking interface. The individual springs were defined by an *ElasticMultiLinear* material model with a CLT stress-strain response characterized by elastic modulus until yield stress, followed by zero strain-hardening until splitting occurs and then by strength degradation until crushing. A *minmax* material was used to define failure at the crushing strain. The base of each spring was fixed, and the top was rigidly connected to the bottom of an *ElasticTimoshenkoBeam* element representing the remaining portion of the CLT panel. Post-tensioned bars were modelled using a *corotational truss* element pinned at the bottom and pin connected to the wall panel at the top. The material model for the post-tensioning bars was defined using *Steel02*. Validation of the modelling approach can be found in [18].

Proper representation of UFPs, including their material models and failure criteria, is crucial because they are the only elements in the PT-CLT wall system that are permitted to undergo nonlinear response under wind loads. Existing numerical models are based on the results of seismic experiments [20, 21]. Such models adopt the *Steel02* material with elastic-perfectly-plastic (EPP) idealizations [20]. However, unlike earthquakes, wind loads have longer durations and several low-amplitude cycles, which can lead to low-cycle fatigue, degradation, and fracture of deformation-controlled elements. Therefore, UFP responses and their design criteria under wind loads can differ from those reported in seismic experimental studies. There is no design or modelling guideline for UFPs in wind response analysis and design. Therefore, in this study, we carried out experimental testing of UFPs under a newly developed set of cyclic wind load protocols.

4 – EXPERIMENTAL TESTING OF UFPs UNDER WIND LOADS

4.1 DEVELOPMENT OF WIND LOAD PROTOCOL

Wind loads have long durations and several low-amplitude cycles for which standardized quasi-static cyclic loading protocols are unavailable. In this study, loading protocols representative of along- and across-wind loads are developed based on nonlinear response history analysis of a 22-story case study mass-timber building equipped with PT-CLT shear walls. The responses of the UFPs in the PT-CLT shear walls were recorded and converted to loading cycles using the rain-flow counting technique [22]. The rainflow counting method, which is widely adopted in fatigue analysis,

https://doi.org/10.52202/080513-0541

converts the random amplitudes from NLRHA results into a group of full and half cycles. The cycle counts at ranges of amplitudes are then used to develop loading sequences. The proposed loading sequences are asymmetric for along-wind loads due to their mean component that subjects the UFPs to accumulating deformation and symmetric for across-wind loads.

Initially, PBWD of the case-study building was carried out according to the design framework in [18]. The case-study building has plan dimensions of 42 m in width and 30 m in depth (Fig. 2). Each story has a height of 3 m, making the total height of the building 66 m. The building is considered to be hypothetically located in Toronto, Canada, and is assumed to serve as office space. Super imposed dead load of 1.5 kPa, live load of 2.4 kPa and snow load of 1kPa on the roof were considered in the design. The structural system consists of CLT floor panels on glulam purlins, supported on glulam beams and columns. Coupled PT-CLT shear walls are the main lateral load-resisting system (LLRS) of the building. The preliminary PBWD results are summarized in Table 1.

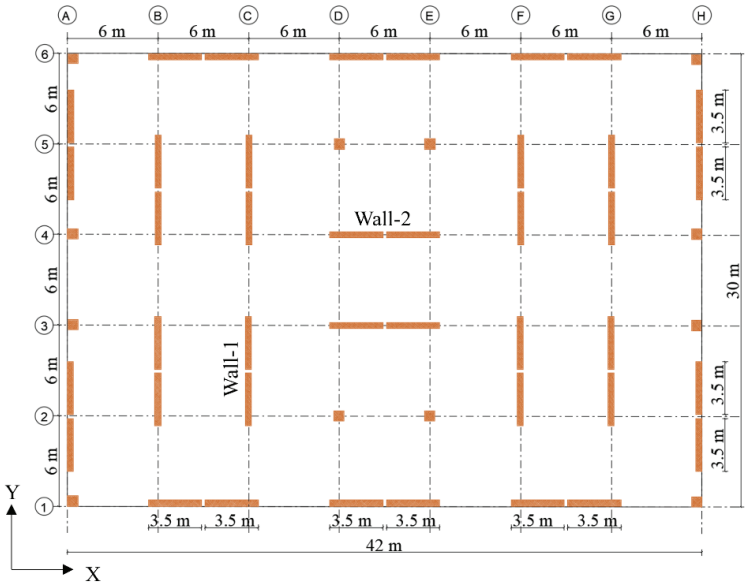

Figure 2. Typical floor layout of a 22-storey prototype mass-timber building with PT-CLT shear walls.

Table 1: Summary of preliminary design results

	X-direction (Across-wind)	**Y-direction (Along-wind)**
CLT cross-section	9-ply E1	9-ply E1
PT bar diameter	32 mm	32 mm
Initial PT force	2316 kN	3474 kN
Number of PT bars	8	12
Number of UFPs	22	34

The building has fundamental periods of 2.2 sec in the first mode (*x-direction translation*) and 1.8 sec in the second mode (*y-direction translation*). Nonlinear response history analysis under floor-by-floor wind loads defined based on wind tunnel test data was conducted. Details of the wind tunnel test are discussed in Section 5.

Global force-deformation hysteresis and roof drift time histories of the structure under design level along- and across-wind loads are shown in Figs. 3(a) and 3(b) and in Figs. 4(a) and 4(b), respectively. The peak roof drifts at the continuous occupancy performance objective were 0.38% and 0.41% in the along- and across- wind direction, respectively, both of which are below the 0.5% limit in the ASCE/SEI PBWD pre-standard [5]. The residual roof drift was also ensured to remain below the 0.1% limit according to the ASCE/SEI PBWD pre-standard. The responses of the UFPs in wall-1 and wall-2 that represent along- and across-wind direction walls, respectively, were also recorded and are shown in Fig. 3(c) and Fig. 4(c). The responses indicate that most of the UFPs in both walls underwent nonlinear deformation under design-level wind.

https://doi.org/10.52202/080513-0541

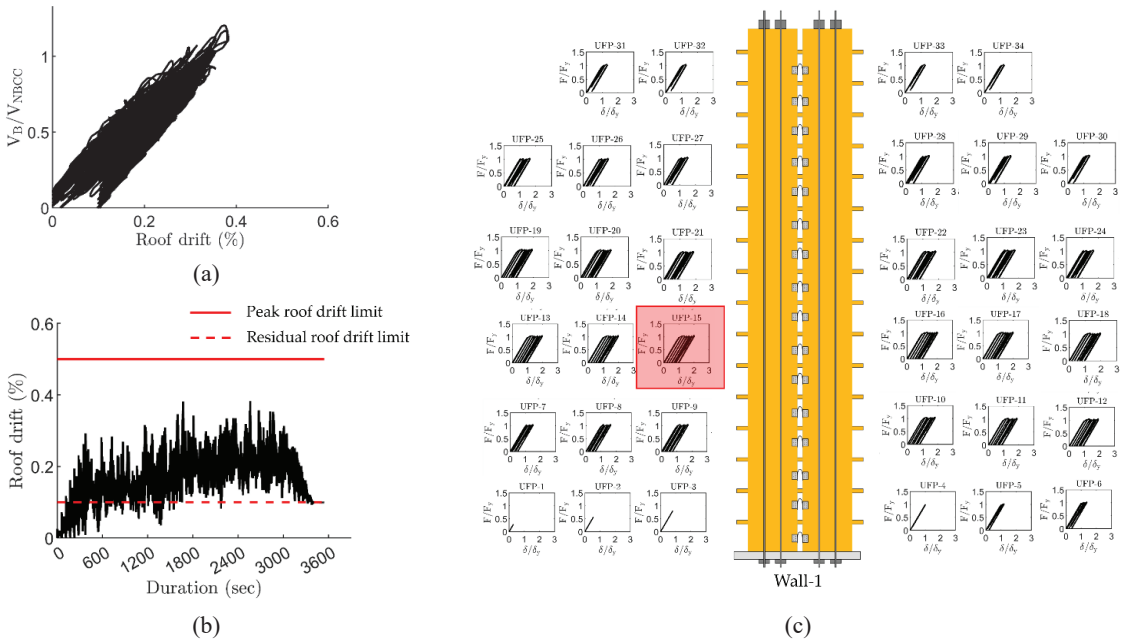

Figure 3. Along-wind response of the prototype building: (a) force-deformation hysteresis; (b) roof drift time history; (c) UFP responses

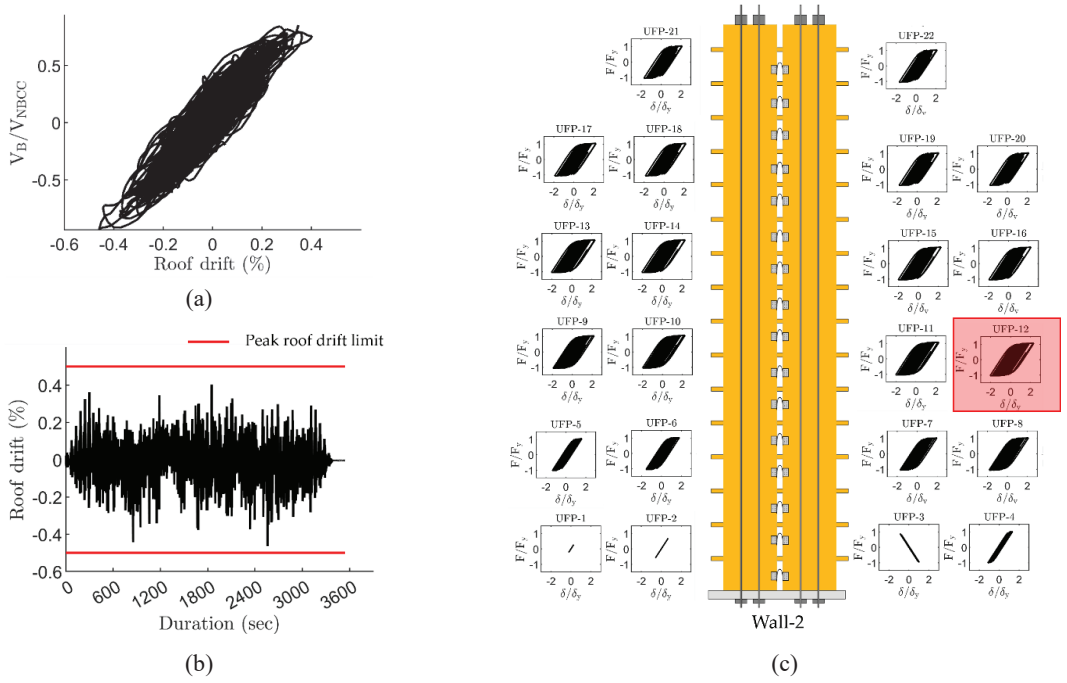

Figure 4. Across-wind response of the prototype building: (a) force-deformation hysteresis; (b) roof drift time history; (c) UFP responses.

According to the recorded UFP responses, the critical UFPs in walls 1 and 2 were the 15th and 12th UFP, respectively. This was due to higher-mode effects in the building causing large deformation around mid-height of the walls. Based on the recorded critical UFP responses, along- and across-wind loading cycles were filtered by implementing the rain-flow counting technique. After the relevant cycles were filtered, the deformation time histories were rounded and sorted for practical purposes.

As shown in Figs. 5(a) and 5(b), the final along- and across-wind loading protocols had 392 and 364 cycles, respectively. Both protocols were defined in terms of the specimen's yield deformation. For the along-wind loading protocol, four mean displacement demands (i.e., $\bar{\delta}_{1-4}$) were determined from the deformation time history and used as additional parameters in defining the loading protocol.

https://doi.org/10.52202/080513-0541

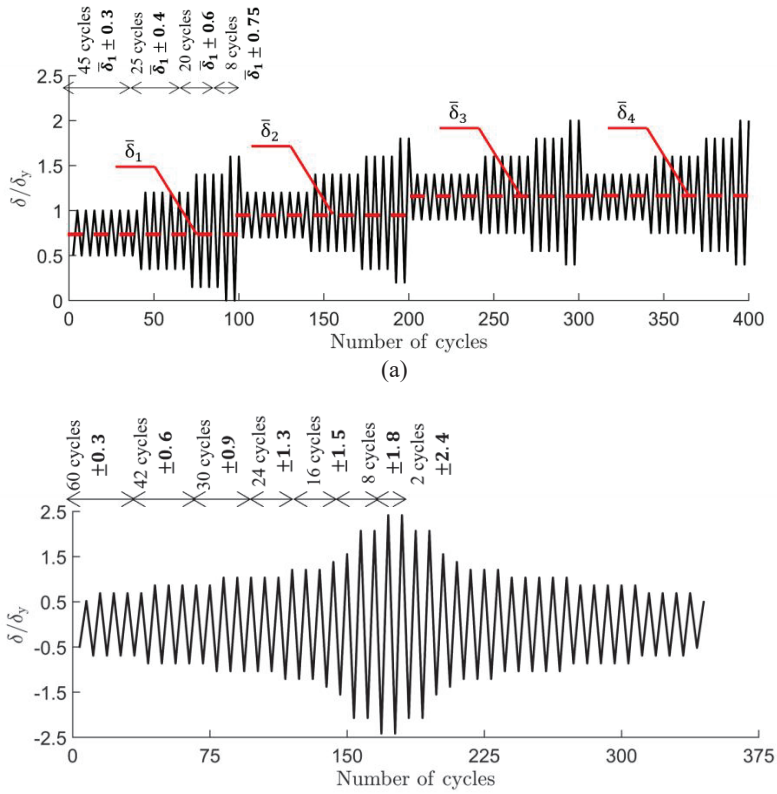

Figure 5. Wind load protocol: (a) along-wind, (b) across-wind

4.2 EXPERIMENTAL TESTING OF UFPs

Experimental tests on UFPs were conducted at Jamieson Structures Laboratory, McGill University, using the wind loading protocols shown in Figs. 5(a) and 5(b). A testing apparatus, shown in Fig. 6(a), was constructed, and the tests were performed using a 1000kN MTS load actuator. Coupled plates were tested simultaneously to ensure that only shear force was applied to the UFPs. A 40-mm-thick steel load plate connected to the UFPs was attached to the testing machine, and the opposite sides of the UFPs were connected to two 12-mm-thick C-section steel braced with two 6-mm C-sections at the top. Two 27-mm-diameter bolts were used to connect the UFPs to the apparatus. Coupon tests were initially conducted to determine the material properties of the specimens, giving a yield stress of 410 MPa and an elastic modulus of 205 GPa. Three sets of UFPs were fabricated from a single parent plate with the same geometry as those used in the prototype building, i.e., 12 mm thick, 150 mm wide, and 55 mm in diameter. The UFPs were tested under monotonic, along-wind, and across-wind loads. Although analytical models exist to estimate the yielding points of UFPs based on material properties, a monotonic test was necessary to determine the overstrength resulting from geometric stiffening, which is not accounted for in existing models. An overstrength factor of 2.2 was observed from the test results. The experimental results for the along-wind and across-wind tests are shown in Figs. 6(b) and 6(c).

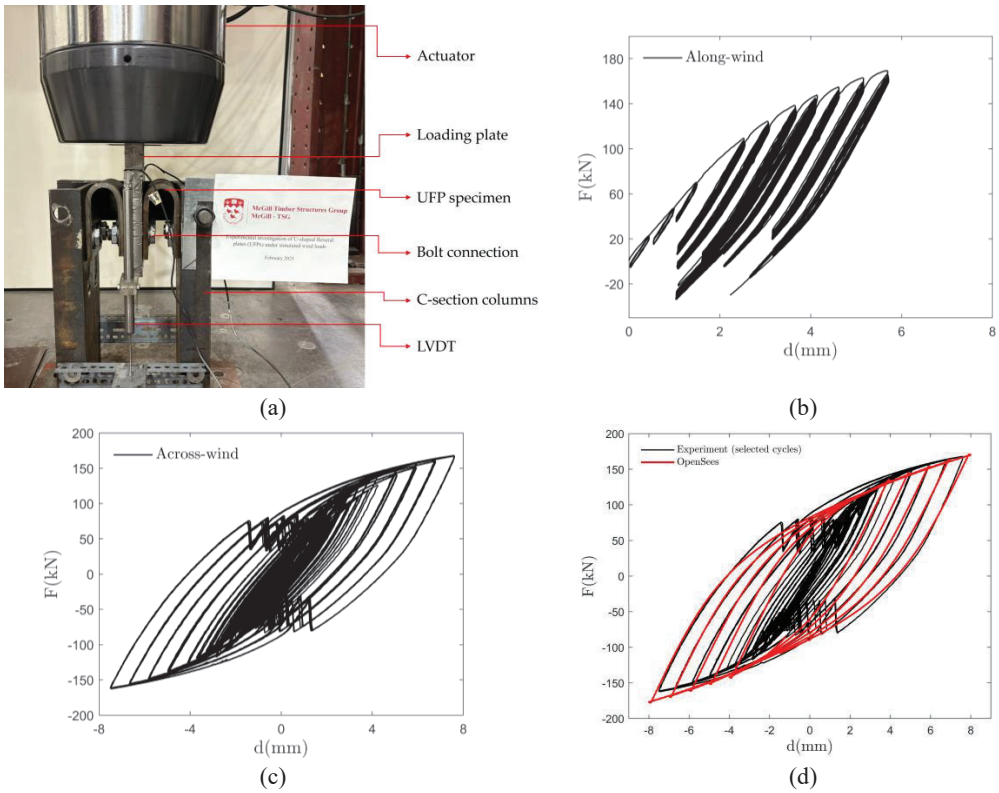

Figure 6. Experimental test results of UFPs under wind loads: (a) test setup; (b) along-wind response; (c) across-wind response; (d) numerical model prediction and experimental result comparison of across-wind response.

The experimental results shown in Figs. 6(b) and 6(c) indicate that the UFPs can resist the anticipated loading without any observable damage. Slippage of bolts in the across-wind test was observed, as shown by the jagged lines in Fig. 6(c). The experimental result revealed that the UFP response does not fit into the EPP idealization that is assumed to be based on seismic loading protocols. Therefore, we calibrated the kinematic hardening parameters to match the results shown in Fig. 6(d) and used them in the numerical model of the prototype building for reliability analysis. The calibrated kinematic hardening parameters for *Steel4* material in *OpenSeesPy* are hardening ratio (b_k) = 0.18 and parameters for exponential transition from linear elastic to hardening asymptote $R_o = 18, r_1 = 0.9$, and $r_2 = 0.15$.

5 – WIND LOAD CHARACTERIZATION

Wind hazard analysis, wind tunnel testing, and directional synthesis of local wind climate and aerodynamic responses are required in PBWD and reliability analysis. The directional hourly mean wind speed record from Toronto Pearson International Airport station was filtered according to the method of independent storms [23] and fitted to the Generalized Extreme Value Distribution (GEVD). Prediction of directional wind speeds with 10-year MRI is shown in Fig. 7(a). The critical wind direction was southwest (250-degree wind angle of attack). The prototype building was oriented with the wide face perpendicular to this direction. A wind tunnel test carried out by Bezabeh et al. [24] on a prismatic model with full-scale dimensions of the prototype building was used to define floor-by-floor aerodynamic load time histories. The test was conducted at the Boundary Layer Wind Tunnel Laboratory (BLWTL), Western University, Canada (Fig. 7(b)). Simultaneous pressures on the building model surface were recorded for 36 wind directions in 10-degree increments. The power spectral densities of along-, across-, and torsional-wind loads are shown in Fig. 7(c). The base load spectrum (S_M) was normalized by the root mean square of the spectrum (σ_m) and the frequency (f) and plotted with the normalized frequency using the building width (B) and the wind speed at the roof height (U_H).

5.1 POD-BASED STOCHASTIC WIND LOAD SIMULATION

Aerodynamic loads obtained from wind tunnel tests are deterministic and hence do not account for the stochastic nature of wind. Therefore, the data-informed proper orthogonal decomposition (POD)-based spectral representation method (SRM) was implemented in this study. The data-informed POD-based SRM method uses wind tunnel-smoothed cross-spectral density as input to calibrate the eigenvalues and eigenvectors of the target load process. For every iteration of the wind reliability analysis, the POD-based SRM generates a unique realization of floor-by-floor load time histories, enabling proper representation of the stochasticity of wind loads.

https://doi.org/10.52202/080513-0541

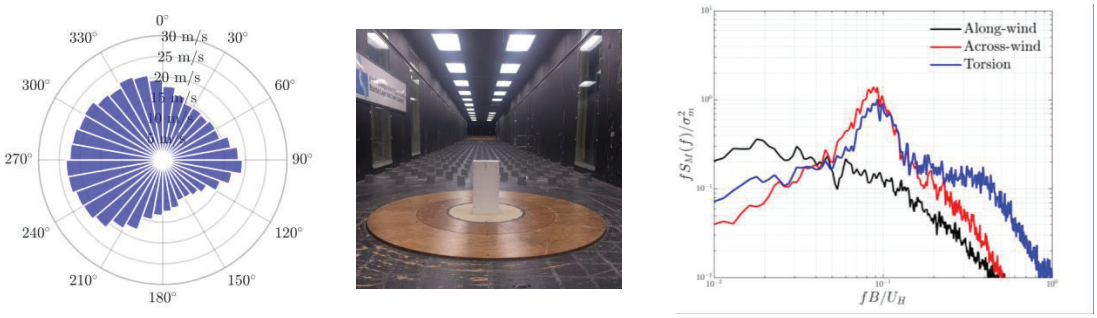

(a) (b) (c)

Figure 7. Wind load characterization: (a) directional 10-year MRI wind speed prediction for Toronto, Canada; (b) aerodynamic wind tunnel testing of the prototype building; (c) normalized along-, across, and torsion-wind PSD.

6 – LIMIT STATE FUNCTIONS

To determine the collapse reliability of the prototype mass-timber building, both system- and component-level limit state functions were considered. At the system level, a 5% inter-storey drift ratio (ISDR) was considered a state of collapse for both along- and across-wind directions. This limit state accounts for the deformation compatibility of the gravity load-resisting systems with the PT-CLT shear walls [25]. At a component level, exceedance of ultimate capacity of the PT bars was considered a collapse limit state. It is known that PT-CLT shear walls derive their overturning moment resistance and recentering capability from PT bars. At yielding of PTs, significant permanent deformation in the overall PT-CLT system can be expected, but the PT bars can take additional load with ductile response. However, at the exceedance of their ultimate capacity, the system loses its overturning moment resistance and becomes prone to imminent collapse. Table 2 summarizes the limit states used in the reliability analysis.

Table 2: Limit state functions for wind reliability analysis

Limit state ID	Criteria
LS-1	System level: Inter-storey drift ratio exceeding 5% in the along-wind direction
LS-2	System level: Inter-storey drift ratio exceeding 5% in the across-wind direction
LS-3	Component level: PT tendons reaching ultimate capacity in the along-wind direction
LS-4	Component level: PT tendons reaching ultimate capacity in the across-wind direction

7 – EFFICIENT STRATIFIED SAMPLING

Crude Monte Carlo sampling poses a large computational demand to propagate structural and load uncertainties in wind reliability analysis [19]. Therefore, stratified sampling, where Monte Carlo simulation is applied only within pre-selected critical strata, was implemented. Because the failure frequency for each limit state is strongly linked with wind speed, it was used as an effective stratification variable. The sample space of wind speeds is partitioned into mutually exclusive and collectively exhaustive strata. The lower bound wind speed of the first stratum is taken as zero, whereas the last stratum is unbounded from above. To define the bounds of each stratum, a constant difference between the square of the lower-bound and upper-bound wind speeds of each stratum was maintained. As discussed in Section 5, the critical wind direction and corresponding probability distribution of wind speeds were determined using the directional hourly mean wind speed record from Environment Canada. Based on this probability distribution fitting for the critical direction, i.e., 250-degree wind, the stratification summarized in Table 3 was implemented in the reliability analysis.

Table 3: Wind speed stratification and number of samples

Strata	Lower bound U (m/s)	Upper bound U (m/s)	Number of samples
1	0	23.1	20
2	23.1	32.5	20
3	32.5	39.6	20
4	39.6	45.7	20
5	45.7	51.1	20
6	51.1	55.9	42
7	55.9	60.4	125
8	60.4	∞	556
	Total		

A preliminary study with a total of 160 equally allocated samples (i.e., 20 samples per stratum) was first carried out to determine the optimal allocation of samples for achieving a target coefficient of variation (COV) of 20%. A total of 823 samples were allocated between the strata to reach accuracy.

Each iteration in the simulation of wind response for reliability analysis accounted for uncertainties in the dynamic properties of the building, gravitational loading, wind climate processing, wind tunnel testing, and numerical modelling. Table 4 lists the corresponding distribution parameters used for these random variables.

https://doi.org/10.52202/080513-0541

Table 4: Uncertainty consideration in reliability analysis

Parameter	Mean	COV	Distribution	Reference
Dead load	D	0.1	Normal	[26]
Live load	L	0.6	Gamma	[26]
Damping	2%	0.3	Lognormal	[27]
Wind hazard	U_H	0.05	Normal	[27]
Wind tunnel test	1	0.075	Truncated Normal	[28]

8 – RESULTS

The probabilities of failure and associated reliability indices, β_{50}, as well as corresponding COVs with respect to the limit states described in Section 6 are reported in Table 5.

Table 5: Failure probabilities and reliability indices

Limit state	P_f	COV	β_{50}
LS-1	1.29×10^{-7}	22.1%	5.15
LS-2	2.07×10^{-7}	20.5%	5.06
LS-3	4.45×10^{-8}	28.2%	5.35
LS-4	6.63×10^{-8}	31.8%	5.28

According to the results shown in Table 5, the prototype mass-timber building exceeds the target reliabilities recommended in ASCE/SEI PBWD pre-standard by 36.0% – 41.9%. This demonstrates the reliability of tall mass-timber buildings equipped with PT-CLT shear walls under wind loads. The final COVs reported in Table 5 differ from the target, i.e., 20%, due to the limitation in the choice of the number of samples used for preliminary study. It is worth noting that a crude MC simulation would require over 200 million samples to reach a failure probability estimation with the same COVs as shown in Table 5. This demonstrates the efficiency of the adopted stratified sampling scheme that required only 823 samples.

9 – SUMMARY AND CONCLUSION

This study conducted a reliability analysis of a 22-storey tall mass-timber building equipped with PT-CLT shear walls as MWFRS. This research implemented a stochastic simulation-based PBWD framework for design and wind reliability analysis of the building. The framework integrated wind load characterization based on wind climate data and wind tunnel testing, a three-dimensional numerical model that utilizes the results of a novel experimental investigation on the deformation-controlled elements of PT-CLT shear walls, stochastically simulated wind loads calibrated based on building-specific wind tunnel data, and an efficient uncertainty propagation scheme. The experimental investigation of UFPs was conducted under newly developed along- and across-wind loading protocols developed based on NLRHA. The results of the experiment demonstrate the distinctive response of UFPs to wind loads, which differs from the current modelling approaches developed based on seismic loading protocols. The results of the reliability analysis demonstrate that PT-CLT shear walls provide robust wind resistance with extremely low collapse probability, and both system- and component-level reliabilities exceed the minimum targets provided in the ASCE/SEI PBWD pre-standard [5].

10 – REFERENCES

[1]. Karacabeyli, E., and Lum, C. (2022). Technical Guide for the Design and Construction of Tall Wood Buildings in Canada. FPInnovations, Pointe-Claire, QC, Canada.

[2]. Bezabeh, M. A., Bitsuamlak, G. T., Popovski, M., Tesfamariam, S. (2018). Probabilistic serviceability-performance assessment of tall mass timber buildings subjected to stochastic wind loads, Part II: Structural reliability analysis. *Journal of Wind Engineering and Industrial Aerodynamics*, 181, 112-125.

[3]. Spence, S. M., and Arunachalam, S. (2022). Performance-based wind engineering: Background and state of the art. *Frontiers in Built Environment*, 8, 830207.

[4]. ASCE/SEI 2019. Pre-Standard for Performance-Based Wind Design. Structural Engineering Institute (SEI), American Society of Civil Engineers.

[5]. ASCE/SEI (ASCE/Structural Engineering Institute) (2023). Pre-Standard for Performance-Based Wind Design V1.1, Reston, VA.

[6]. Vickery, B. J. (1970). Wind action on simple yielding structures. *Journal of the Engineering Mechanics Division*, 96(2), 107-120.

[7]. Wyatt, T. A., May, H. (1971). The ultimate load behaviour of structures under wind loading. In *Proceedings of the 3rd International Conference on Wind Effects on Buildings and Structures*, Tokyo, Japan.

[8]. Tschanz, T., Davenport, A. G. (1983). The base balance technique for the determination of dynamic wind loads. *Journal of Wind Engineering and Industrial Aerodynamics*, 13(1-3), 429-439.

[9]. Georgiou, P. N., Vickery, B. J., & Surry, D. (1988). The effect of non-linear structural behavior on wind-induced plastic damage of low-rise buildings. *Journal of Wind Engineering and Industrial Aerodynamics*, 29(1), 235-244.

[10]. Chen, D., Davenport, A. G. (2000). Vulnerability of tall buildings in typhoons. *Advances in Structural Dynamics*, 2, 1455-1462.

[11]. Hong, H. P. (2004). Accumulation of wind-induced damage on bilinear SDOF systems. *Wind and Structures*, 7(3), 145-158.

[12]. Petrini, F., and Ciampoli, M. (2012). Performance-based wind design of tall buildings. *Structure and Infrastructure Engineering*, 8(10), 954-966.

[13]. Ciampoli, M., Petrini, F., and Augusti, G. (2011). Performance-based wind engineering: Towards a general procedure. *Structural Safety*, 33(6), 367-378.

https://doi.org/10.52202/080513-0541

[14]. Spence, S. M. J., Chuang, W. C., Tabbuso, P., Bernardini, E., Kareem, A., Palizzolo, L., and Pirrotta, A. (2016). Performance-based engineering of wind-excited structures: A general methodology. In *Geotechnical and Structural Engineering Congress 2016*, Phoenix, Arizona, USA. pp. 1269-1282.
[15]. Bezabeh, M.A., Bitsuamlak, G.T., and Tesfamariam, S. (2020). Performance-based wind design of tall buildings: Concepts, frameworks, and opportunities. *Wind and Structures*, 31(2), 103–142.
[16]. American Society of Civil Engineers. (2017, June). Minimum design loads and associated criteria for buildings and other structures.
[17]. Chuang, W. C., and Spence, S. M. (2020). Probabilistic performance assessment of inelastic wind excited structures within the setting of distributed plasticity. *Structural Safety*, 84, 101923.
[18]. Berile, N. K., & Bezabeh, M. A. (2025). Performance-based wind design of tall mass timber buildings with coupled post-tensioned cross-laminated timber shear walls. *Journal of Wind Engineering and Industrial Aerodynamics*, *257*, 105981.
[19]. Arunachalam, S., & Spence, S. M. (2023). An efficient stratified sampling scheme for the simultaneous estimation of small failure probabilities in wind engineering applications. *Structural Safety*, *101*, 102310.
[20]. Iqbal, A., Pampanin, S., Palermo, A., Buchanan, A.H. (2015). Performance and design of LVL walls coupled with UFP dissipators. *J Earthq Eng* 2015;19(3):383–409.
[21]. Pei, S., van de Lindt, J. W., Barbosa, A. R., Berman, J. W., McDonnell, E., Daniel Dolan, J., Blomgren, H.-E., Zimmerman, R. B., Huang, D., & Wichman, S. (2019). Experimental seismic response of a resilient 2-story mass-timber building with post-tensioned rocking walls. *Journal of Structural Engineering*, 145(11), 04019120. https://doi.org/10.1061/(ASCE)ST.1943-541X.0002382.
[22]. Amzallag, C., Gerey, J. P., Robert, J. L., & Bahuaud, J. (1994). Standardization of the rainflow counting method for fatigue analysis. *International Journal of Fatigue*, *16*(4), 287-293.
[23]. Cook, N. J. (1982). Towards better estimation of extreme winds. *J. Wind Eng. Ind. Aerod.* 9(1982): 295−323.
[24]. Bezabeh, M. A., Bitsuamlak, G. T., Popovski, M., & Tesfamariam, S. (2020). Dynamic response of tall mass-timber buildings to wind excitation. *Journal of Structural Engineering*, 146(10), 04020199.
[25]. Wichman, S., 2023. Seismic Behavior of Tall Rocking Mass Timber Walls. PhD Thesis. University of Washington, Seattle, USA.
[26]. Zhang, H., Ellingwood, B. R., & Rasmussen, K. J. (2014). System reliabilities in steel structural frame design by inelastic analysis. *Engineering Structures*, *81*, 341-348.
[27]. Bashor, R., Kijewski-Correa, T., & Kareem, A. (2005, May). On the wind-induced response of tall buildings: The effect of uncertainties in dynamic properties and human comfort thresholds. In *Proceedings of Americas Conference on Wind Engineering,* Baton Rouge, LA (Vol. 31).
[28]. Bernardini, E., Spence, S. M., Kwon, D. K., & Kareem, A. (2015). Performance-based design of high-rise buildings for occupant comfort. *Journal of Structural Engineering*, *141*(10), 04014244.